Metal-Substituted Bacteriochlorophylls. 2. Changes in Redox Potentials and Electronic Transition Energies Are Dominated by Intramolecular Electrostatic Interactions

Dror Noy,[†,‡,⊥] Leszek Fiedor,[†,§,⊥] Gerhard Hartwich,[∥,⊗] Hugo Scheer,[∥] and Avigdor Scherz*[,†]

Department of Plant Sciences, Weizmann Institute of Science, 76100 Rehovot, Israel, Botanisches Institut der Universität, D-80638 München, Germany, and Institute für Physikalische und Theoretische Chemie, TU München, D-85748, Garching, Germany

Received March 19, 1997

Abstract: Changes in the electronic transition energies and redox potentials because of metal substitution in bacteriochlorophyll a justify the recently suggested correlation between electronegativity χ_M, covalent radius, and an effective charge, Q_M, at the metal atom center. A simple electrostatic theory in which Q_M modifies the energies of the frontier molecular orbitals by Coulombic interactions with the charge densities at the atomic π centers is suggested. The relative change in electrostatic potential at a distance r_a from the metal center is $\Delta Q_M/r_a$, where ΔQ_M, the change in the metal effective positive charge because of Mg being substituted by another metal, varies with the change in metal electronegativity (Mulliken's values) $\Delta\chi_M$ and covalent radius Δr_M^c. ΔQ_M consists of two components: the major component, ΔQ_M^o, characteristic of the central metal, is independent of the molecular environment and proportional to the electronegativity of the metal at a typical valence state. The second component, $\Delta q_{M,N}$, reflects those perturbations induced by the molecular frame. It depends on the overlap between the metal and ligand orbitals hence changes both with the metal covalent radius (*i.e.*, its typical "size") and the particular orbital environment. For the series of metals that we examined, we determined that $\Delta Q_M^o = (0.12 \pm 0.02)\,\Delta\chi_M$. Significant contributions of $\Delta q_{M,N}$ to $\Delta Q_{M,N}$ were found for the changes in the energies of the *y*-polarized electronic transitions B_y and Q_y and to a lesser extent the first oxidation potential E_{Ox}^1. Minor contributions were found for the changes in the energies of the *x*-polarized electronic transitions B_x and Q_x and the first reduction potential E_{Red}^1. The model agrees well with target testing factor analysis performed on the entire data space. Simulations of the experimental redox potentials and the four electronic transitions required mixing of single-electron promotions; however, the coefficients for the configuration interactions were assumed to be metal-independent within the examined series because the relative oscillator strengths of the various transitions did not show significant changes upon metal substitution. The reported observations and the accompanying calculations provide experimental support to the modern concepts of electronegativity and may help in better understanding biological redox centers consisting of porphyrins or chlorophylls.

Introduction

Electronegativity is an important part of the intuitive approach that helps chemists in understanding nature. In particular, it provides a measure to the uneven distribution of electrons among bound atoms and the probability of electron transfer among two unbound atoms (or molecules). Still, the formulation of both atom and group electronegativity values in terms of fundamental atomic forces is problematic.[1] Such a formulation could provide new insight to inter- and intramolecular electron transfer both in the ground and excited states of complex biological systems, keeping in mind that group electronegativity describes the power of a system to attract an electron based on the properties of individual chemical components (atoms or chemical groups).

Complexes of proteins with chlorophyll (Chl), bacteriochlorophyll (BChl), and D_{4h} porphyrin are the key players in fundamental biological electron transfer reactions.[2−4] Their in situ redox potentials (RP) and electronic transition energies (TE) are finely tuned to their function as electron donors, acceptors, or light-harvesting units. Yet, despite extensive research, the mechanism behind this tuning is still not understood. For example, there is no rigorous explanation for the difference in oxidation potentials of the Chls in P680 and P700, the primary electron donors of photosystems II and I, respectively. Model systems with systematically modified RP and TE are useful for resolving this mechanism. Such modifications were introduced by metal substitution in the porphyrin or Chl macrocycle. The observed linear relationships between the porphyrin RP and the metal electronegativities, which are in line with the concept of group electronegativity, could shed light upon the control mechanisms of redox reactions in biological complexes and link

* Author to whom correspondence should be addressed.
† Weizmann Institute of Science.
‡ In partial fulfillment of M.Sc. Thesis.
§ Present address: Institute of Molecular Biology, Jagiellonian University, PL-31-120 Crakow, Poland.
⊥ In partial fulfillment of Ph.D. Thesis.
∥ Botanisches Institut der Universität.
⊗ Institute für Physikalische und Theoretische Chemie.

(1) Mullay, J. In *Structure and Bonding*; Sen, K. D., Jørgensen, C. K., Eds.; Springer-Verlag: Berlin, 1987; Vol. 66, pp 1−25.
(2) Moser, C. C.; Page, C. C.; Farid, R.; Dutton, P. L. *J. Bioenerget. Biomembranes* **1995**, *27*, 263−274.
(3) Nugent, J. H. A. *Eur. J. Biochem.* **1996**, *237*, 519−531.
(4) Franzen, S.; Martin, J. L. *Ann. Rev. Phys. Chem.* **1995**, *46*, 453−487.

S0002-7863(97)00875-5 CCC: $15.00
Published on Web 04/01/1998

the electronegativity of individual metal atoms with fundamental physical forces.

Redox reactions and the major electronic transitions in porphyrins and Chls occur within the two highest occupied and lowest unoccupied molecular orbitals. Extensive theoretical studies by Gouterman and others[5−11] have indicated that the wavelengths of the four major electronic transitions in porphyrins (Q_y, Q_x, B_x, and B_y; in order of increasing energy) are determined by the energies of the lowest unoccupied molecular orbitals (LUMO and LUMO+1), along with the relative energies of the highest occupied molecular orbital (HOMO and HOMO-1). The energies of HOMO and LUMO also determine the potentials of ring-centered porphyrin oxidation and reduction. Therefore, observed metal effects were thought to reflect modifications of charge densities in the LUMO and HOMO induced by the electronegativity of the metal.[6,12−15] According to Gouterman,[6] changes in the π electron density can result from two alternative mechanisms: (a) modifying the electric potential at the nitrogen's σ electrons, which then leads to electron flow to or from the macrocycle toward the metal (inductive effect), and (b) mixing the metal d orbitals with the π orbitals of the macrocycle (conjugative effect). Although Gouterman suggested the predominance of the conjugative effect, most of his followers adopted the first mechanism, which could account for the observed trends in RP of metal-substituted porphyrins or Chls[12] but failed by more than an order of magnitude to predict the experimental results quantitatively.[13] Furthermore, no clear connection was suggested between metal substitution in vitro and the in vivo modification of pigment environment.

One particular obstacle for semiempirical calculations of the frontier molecular orbitals in porphyrins and, to a lesser extent, in metal-substituted Chl a ([M]-Chl)[16,17] is the strong overlap of the different optical transitions, even in metallochlorins. Tetrahydroporphyrins, such as BChl, have the advantage of relatively well-resolved electronic transitions. Unfortunately, the few metal-substituted BChls ([M]-BChls) that were synthesized so far[18,19] did not provide sufficient information to enable a systematic study of the metal effect on the frontier orbitals. Hence, we set out to explore different avenues for further metalation of bacteriopheophytin (BPhe). Initially, we had developed mild methods for inserting Zn(II), Cu(II), and Cd(II) into the BPhe and derivatives.[20−23] Later, we developed a procedure for transmetalation of [Cd]-BChl with other divalent metals, such as Co(II), Pd(II), Mn(II), and Ni(II).[22] The TE of the M-BChls were found to be linearly related to the metal electronegativities according to Pauling (χ_M^P), if the [M]-BChls were grouped according to an experimental or putative coordination state. Even better correlation was obtained if χ_M^P was divided by r_M^i, the metal ionic radius. Additional data concerning the RP of [M]-BChls was provided by Geskes et al.[24] and Renner et al.,[25] who conducted the first voltammetric measurements in tetrahydrofuran (THF). The linear correlation of the RP values with χ_M^P/r_M^i was fairly good but somewhat less satisfactory than with the previously mentioned spectroscopic data.[22] Furthermore, [M]-BChls seemed to be in some mixed coordination or aggregation state. This could be partly due to mixed coordination states of some [M]-BChls in THF or aggregate formation.

The observed spectra and RP of [M]-Chls were explained by the same inductive mechanisms as previously proposed for D_{4h} porphyrins.[12−14] However, the data of Geskes et al.[24] as well as our spectroscopic data[22] are not in line with predictions that follow these models. In particular, Gouterman[6] suggested that both the inductive and conjugative effects rely on the high electron densities in the nitrogens of the involved orbitals. Hence, in D_{4h} porphyrins a strong metal effect is expected for the a_{2u} (HOMO) and $e_{gx,y}$ (LUMO and LUMO+1) orbitals, but not for the a_{1u} orbital (HOMO-1). In [M]-BChls, a_{1u} and e_{gy} are significantly lifted above a_{2u} and e_{gx}, respectively,[26] and become HOMO and LUMO+1. Thus oxidation involves an ionization of a_{1u}, whereas reduction involves an electron addition to the (virtual) e_{gx} orbital.[27] Using the suggested scheme for D_{4h} porphyrins, the oxidation potential should then undergo only minor variations upon metal exchange in both [M]-Chls and [M]-BChls, whereas the reduction potential should depend more strongly on the metal electronegativities. The experimental studies of Geskes et al.[24] did not agree with this expected behavior: despite the major difference in π-electron distribution at their nitrogen positions,[5,8,26] the energy change of the a_{1u} orbital was almost the same as that of the e_{gx} orbital. The concept of the inductive/conjugative effect is also in contrast with the spectral data for both [M]-Chls[11,16] and [M]-BChls:[22] the Q_y TE should be strongly modified upon metal substitution if the energy of a_{1u} is much less sensitive to metal variations than that of e_{gx}. In practice, the shift of the Q_y band is only 20% of the Q_x band shift. Discrepancies between predictions and observations in [M]-BChls were seen for oscillator strengths as well: no significant changes in the oscillator strengths accompanied a profound shift of the Q_x TE in [M]-Chls and [M]-BChls. Note that the oscillator strengths did vary in metal-substituted tetraphenylporphyrins,[6,7,13] octaethylporphyrins,[13] and peripherally substituted octaethylporphyrins.[28] The analysis is

(5) Petke, J. D.; Maggiora, G. M.; Shipman, L. L.; Christoffersen, R. E. *Photochem. Photobiol.* **1980**, *32*, 399−414.
(6) Gouterman, M. *J. Chem. Phys.* **1959**, *30*, 1139−1161.
(7) Gouterman, M. *J. Mol. Spectrosc.* **1961**, *6*, 138−163.
(8) Gouterman, M.; Wagniere, G. H.; Snyder, L. C. *J. Mol. Spectrosc.* **1963**, *11*, 108−127.
(9) Zerner, M.; Gouterman, M. *Theoret. Chim. Acta* **1966**, *4*, 44−63.
(10) Thompson, M. A.; Fajer, J. *J. Phys. Chem.* **1992**, *96*, 2933−2935.
(11) Warshel, A.; Parson, W. W. *J. Am. Chem. Soc.* **1987**, *109*, 6143−6152.
(12) Fuhrhop, J. H. In *Porphyrins and Metalloporphyrins*; Smith, K. M., Ed.; Elsevier: Amsterdam, 1975; pp 593−623.
(13) Fuhrhop, J. H.; Kadish, K. M.; Davis, D. G. *J. Am. Chem. Soc.* **1973**, *95*, 5140−5147.
(14) Kadish, K. M.; Bottomely, L. A.; Kelly, S.; Schaeper, D.; Shiue, L. R. *Bioelectrochem. Bioenerget.* **1981**, *8*, 213−222.
(15) Napa, M.; Valentine, J. S. *J. Am. Chem. Soc.* **1978**, *100*, 5075−5080.
(16) Watanabe, T.; Machida, K.; Suzuki, H.; Kobayashi, M.; Honda, K. *Coord. Chem. Rev.* **1985**, *64*, 207−224.
(17) Watanabe, T. In *Chlorophylls*; Scheer, H., Ed.; CRC Press: Boca Raton, FL, 1991; pp 287−315.
(18) Fajer, J.; Brune, D. C.; Davis, M. S.; Forman, A.; Spaulding, L. D. *Proc. Natl. Acad. Sci. U.S.A.* **1975**, *72*, 4956−4960.
(19) Donhoe, R. J.; Frank, H. A.; Bocian, D. F. *Photochem. Photobiol.* **1988**, *48*, 531−537.
(20) Fiedor, L. Ph.D. Thesis, Weizmann Institute of Science, 1994.
(21) Hartwich, G.; Scheer, H.; Salomon, Y.; Brandis, A.; Scherz, A. Patent, in press.
(22) Hartwich, G.; Fiedor, L.; Katheder, I.; Cmiel, E.; Schäfer, W.; Noy, D.; Scherz, A.; Scheer, H. *J. Am. Chem. Soc.* **1998**, *120*, 3675−3683.
(23) Hartwich, G. Ph.D. Thesis, Technical University, Munich, 1994.
(24) Geskes, C.; Hartwich, G.; Scheer, H.; Mäntele, W.; Heinze, J. *J. Am. Chem. Soc.* **1995**, *117*, 7776−7783.
(25) Renner, M. W.; Zhang, Y.; Noy, D.; Scherz, A.; Smith, K. M.; Fajer, J. In *The Reaction Center of Photosynthetic Bacteria. Structure and Dynamics*; Michel-Beyerle, M. E., Ed.; Springer-Verlag: Berlin, 1996; pp 369−380.
(26) Hanson, L. K. In *Chlorophylls*; Scheer, H., Ed.; CRC Press: Boca Raton, FL, 1991; pp 993−1014.
(27) For clarity, we keep the porphyrin's D_{4h} notation although the a_{2u}, a_{1u}, e_{gx}, and e_{gy} orbitals of porphyrins become b_{1u}, a_u, b_{2g}, and b_{3g}, respectively, in D_{2h} tetrahydroporphyrins.
(28) Binstead, R. A.; Crossley, J. M.; Hush, N. S. *Inorg. Chem.* **1991**, *30*, 1259−1264.

further complicated by the fact that the Q_x but not the Q_y TE are strongly dependent on the coordination of the metal.[22]

In light of these considerations we examined alternative explanations for the correlation between the electronegativity of the central metal and the orbital energies in [M]-Chls and [M]-BChls. Data presented in the preceding paper[22] suggested that incorporating metals with different electronegativities changes the effective positive charge in the center of the BChl macrocycle and therefore the energy of the individual π orbitals. We also proposed that this charge is inversely proportional to a corrected electronegativity, which is given by χ_M^P/r_M^i, where r_M^i, the metal ionic radius, is a function of the metal coordination number.[29] Here we attempt to provide a rigorous evaluation of this somewhat intuitive explanation. First, the metal electronegativity (according to Mulliken) is expressed in terms of effective positive charges. Then it is shown that the electrostatic interaction between these charges and the electron density of each π center in the frontier molecular orbitals changes the orbital energies, resulting in the observed modified RP and TE. To simplify the theoretical considerations, the examination was focused only on macrocycle redox reactions (ring centered) and electronic transitions of [M]-BChls with not more than one axial ligand. New measurements in acetonitrile solution containing 10% dimethylformamide (AN/DMF) provided the redox potentials of the selected [M]-BChl and the corresponding spectroscopic data. These measurements were conducted because [M]-BChl does not aggregate in this solvent system and the metals are tetra- or at most pentacoordinated.[20] Finally, the calculated positive charge at the [M]-BChl center was found to be linearly correlated with the metal electronegativity (according to Pauling) divided by the metal ionic radius.

Theoretical Considerations

Relationship between Metal Electronegativity and Electrostatic Potentials. The Pauling scale of electronegativity refers to an average valence and coordination state of the individual atoms. Obviously, "The power of an atom in a molecule to attract electrons to itself" [30] depends upon its molecular environment including state of coordination and valence. Therefore, it is not surprising that the linear correlation between the TE and χ_M^P of atom "M" in [M]-BChls was improved after grouping the molecules according to their putative coordination number. The same is true for the need to divide χ_M^P by r_M^i, which increases with the number of ligands: the ionic radius in transition metals is inversely proportional to the coordination number,[29] reflecting the electron density around the nuclei and subsequently the atom electronegativity.[1] Mulliken's definition of electronegativity being half the sum of the electron affinity and ionization potential explicitly takes into account the valence state of the atom in a molecule.[1,31] Because of limited experimental data, Mulliken's electronegativity values could not be calculated for many transition metals. However, the idea that the electronegativity of an atom in molecules depends on its valence, state of coordination, etc. has proven to be very useful and will be applied here. Another definition of electronegativity was introduced by Gordy,[32] who suggested that it is the electrostatic potential $V(Q_M, r_M^c)$, created at the atom's covalent radius r_M^c because of its effective nuclear charge Q_M. These concepts gained theoretical support from density functional theory (DFT). Parr et al.[33] have identified Mulliken's definition of electronegativity with the electronic chemical potential, whereas Politzer et al.[34] have provided theoretical justification to Gordy's approach. They showed that r_M^c is linearly correlated with r_M^μ, the radius at which the electrostatic potential of an atom equals its electronic chemical potential

$$r_M^\mu = \alpha r_M^c + \beta \tag{1}$$

where α and β are semiempirical correlation factors. Hence, $V(Q_M, r_M^\mu)$ is given by

$$V(Q_M, r_M^\mu) = Q_M/r_M^\mu \tag{2}$$

where Q_M is the effective atomic charge due to the nuclear charge screened by the electron density at $r_a < r_M^\mu$. A linear correlation was found between Mulliken's electronegativity values (χ_M) of 25 atoms and their theoretical $V(Q_M, r_M^\mu)$ values

$$V(Q_M, r_M^\mu) = \gamma\chi_M + \delta \tag{3}$$

where, again, γ and δ are the semiempirical correlation coefficients. Alonso and Balbas[35] determined that the parameters α, β, γ, and δ in eqs 1 and 3 equal 0.55, 0.75, 0.33, and 0.22, respectively, for isolated atoms.[36] The intramolecular values of these parameters are probably different.[37]

At distances r_a larger than r_M^μ, the electrostatic potential is given by

$$V(Q_M, r_a > r_M^\mu) = Q_M/r_a \tag{4}$$

where the effective atomic charge is given by combining eqs 1, 2, and 3

$$Q_M = (\alpha r_M^c + \beta)(\gamma\chi_M + \delta) \tag{5}$$

If the electronegativity of the incorporated metal relative to Mg is

$$\Delta\chi_M \equiv \chi_M - \chi_{Mg} \tag{6}$$

then, the change in charge, ΔQ_M, at a BChl molecule center because of metal substitution is given, to a first-order approximation, by

$$\Delta Q_M = \Gamma\Delta\chi_M + \Lambda\Delta r_M^c \tag{7a}$$

where

$$\Gamma = (\alpha\gamma r_{Mg}^c + \beta\gamma) \tag{7b}$$

(29) Cotton, F. A.; Wilkinson, G. *Advanced Inorganic Chemistry*, 5th ed.; Wiley: New York, 1988.

(30) Pauling, L. *The nature of the chemical bond*; Cornell University Press: New York, 1939.

(31) Bratsch, S. G. *J. Chem. Educ.* **1988**, *65*, 34−41.

(32) Gordy, W. *Phys. Rev.* **1946**, *69*, 604−607.

(33) Parr, R. G.; Donnely, R. A.; Levy, M.; Palke, W. E. *J. Chem. Phys.* **1978**, *68*, 3801−3807.

(34) Politzer, P.; Parr, R. G.; Murphy, D. R. *J. Chem. Phys.* **1983**, *79*, 3859−3861.

(35) Alonso, J. A.; Balbás, L. C. In *Structure and Bonding*; Sen, K. D., Jørgensen, C. K., Eds.; Springer-Verlag: Berlin, 1987; Vol. 66, pp 41−78.

(36) The original values are 0.55, 1.42, 4.72, and 0.12. The present parameters are converted from the original atomic units coordinates into a system where r^c and r^μ are measured in Å, χ in eV, and Q in electron charge units.

(37) Liu, G. H.; Parr, R. G. *J. Am. Chem. Soc.* **1995**, *117*, 3179−3188.

and

$$\Lambda = (\alpha\gamma\chi_{Mg} + \alpha\delta) \tag{7c}$$

Hence, a change in the metal's effective charge is a function of both its electronegativity and covalent radius. Conversely, if TE and RP are functions of an effective positive charge at the molecule center, they cannot be linearly correlated with χ_M of [M]-BChls, unless r_M^c is the same for all studied metals (which is not the case for our studied series of metals). A change of ΔQ_M at the center of the molecule modifies the energy of an electron density $\rho(r_a)$ at a distance r_a from the molecule center by

$$\Delta E_{M,\rho} = \frac{-\Delta Q_M \rho(r_a)}{r_a} \tag{8a}$$

and the effect of ΔQ_M on the energy level of a MO, ϕ_n with an electron distribution, $\rho_n(r_a)$ is given by

$$\Delta E_{M,n} = -\Delta Q_M \int_0^\infty \frac{\rho_n(r_a)}{r_a}\, dr_a = \Delta Q_M V_n^{eff} \tag{8b}$$

Metal Effects on the Energies of the Electronic Transitions. The following assumptions were made in predicting the metal effect on the energy of the frontier orbitals of [M]-BChls: (1) A frontier MO, ϕ_n, is given by

$$\phi_n = \sum_{a=1}^{24} \Phi_{a,n}\theta_a \tag{9}$$

where $\Phi_{a,n}$ is the coefficient of the nth MO at atom "a" and θ_a is the p_z orbital of atom "a" (this representation includes the conjugated π centers of the BPhe macrocycle as well as the C-3 acetyl and C-13^2 keto groups). In the porphyrin macrocycle, each atom contributes one π electron to the molecular π system except for two pyrrolenine-type nitrogens (N22, N24), which contribute two electrons each. An electron that joins a π MO leaves behind one positive charge that is equally shared among the π centers. For 20 carbon and four nitrogen π centers, there are 26 such positive charges. In practice, the positive charges can be displaced toward the molecule's peripheral groups through the σ bonds. Taking this into account and approximating the electron density on atom "a" by $(\Phi_{a,n})^2$, we obtained the following approximation for the effective electron distribution in the MO ϕ_n

$$\rho_n(r_a) \approx \rho_{a,n} = (\Phi_{a,n})^2 - \frac{\kappa_a}{26Z_a} \tag{10a}$$

where κ_a equals 2 for the pyrrolenine type nitrogens (see above) and 1 for all the other atoms in the π system. Z_a is an empirical parameter that accounts for the actual σ-electron distribution. Thus, the integral in eq 8b becomes a sum over the conjugated π centers

$$V_n^{eff} = \sum_a \frac{\rho_{a,n}}{r_a} \tag{10b}$$

(2) We showed in the preceding paper[22] that the difference between the lowest singlet and triplet excited states is independent of the incorporated metal. Hence, we have assumed that the exchange and Coulombic integrals, K and J, respectively, are independent of ΔQ_M. Thus hybridization is not changed by central metal substitution. A similar assumption was recently made in calculating the energies of frontier MOs of β-substituted tetraphenylporphyrins.[28] (3) The electron density at each π center is not modified by metal substitution. Specifically, the metal changes the BChl Hamiltonian, but the charge densities at the individual atoms of the HOMOs and LUMOs, composed of p_z orbitals, are indifferent to the substituted metal. Nonetheless, using the principle of electronegativity equalization,[35,38] σ electrons probably migrate toward the metal. This electron migration may affect its Γ and Λ values, which should reflect the effect of the molecular environment on the atom electronegativity.[37] With these considerations and combining eqs 7, 8, and 10, metal substitution in BChl is expected to modify the energy of the nth frontier MO by

$$\Delta E_{M,n} = \Delta Q_M V_n^{eff} \approx (\Gamma\Delta\chi_M + \Lambda\Delta r_M^c)\sum_a \frac{\rho_{a,n}}{r_a} \tag{11a}$$

Hence, the change in the energy of a single electron promotion ij is

$$\Delta E_{M,ij} = (V_j^{eff} - V_i^{eff})\Delta Q_M \tag{11b}$$

(4) As originally proposed by Gouterman,[6] reasonable representations of the four electronic transitions to the lowest excited states of BChl and its metal derivatives are provided by linear combinations of the single electron promotions from the HOMOs to the two LUMOs weighted by the configuration interaction (CI) coefficients C_{ij}[5,10,11]

$$\Psi_{Q_y} = C_{23}\psi_{23} - C_{14}\psi_{14} \tag{12}$$

$$\Psi_{B_y} = C_{14}\psi_{23} + C_{23}\psi_{14}$$

$$\Psi_{Q_x} = C_{13}\psi_{13} + C_{24}\psi_{24}$$

$$\Psi_{B_x} = -C_{24}\psi_{13} + C_{13}\psi_{24}$$

where $\psi_{ij} \equiv \phi_i \rightarrow \phi_j$.

Assuming that J and K are constant and following Foresman et al.,[39] the energy of an electronic transition "T" is given by

$$\Delta E_{M,T} = \sum_{ij} C_{ij,T}^2 \Delta E_{M,ij} \tag{13a}$$

Since the relative oscillator strengths of the four electronic transitions are insensitive to the incorporated metal, the C_{ij} coefficients are considered to be the same for all examined compounds. Substituting eq 11b into 13a yields the predicted shift of the electronic transition "T"

$$\Delta E_{M,T} = V_T^{eff}\Delta Q_M \approx V_T^{eff}(\Gamma\Delta\chi_M + \Lambda\Delta r_M^c) \tag{13b}$$

where $V_T^{eff} \equiv \sum_{ij} C_{ij,T}^2 (V_j^{eff} - V_i^{eff})$.

Metal Effect on the Redox Potentials. The Koopman theorem states that the vertical ionization energy (I) equals the negative Hartree−Fock (HF) energy of the molecular orbital ϕ_i from which the electron has been removed.[39,40] A symmetrical statement is given for the electron affinity (A) and the lowest unoccupied MO, ϕ_{i+1}. Hence, changes in ionization potentials

(38) Sanderson, R. T. *J. Chem. Educ.* **1954**, *31*, 2−7.
(39) Foresman, J. B.; Head-Gordon, M.; Pople, J. A.; Frisch, M. J. *J. Phys. Chem.* **1992**, *96*, 135−149.
(40) Levine, I. *Quantum chemistry*, 4th ed.; Prentice Hall: Englwood Cliffs, NJ, 1991.

and electron affinity of [M]-BChl, ΔI_M and ΔA_M, respectively, are given by

$$\Delta I_M = -(E_{M,HOMO} - E_{Mg,HOMO}) = -\Delta E_{M,HOMO} \quad (14a)$$

$$\Delta A_M = -(E_{M,LUMO} - E_{Mg,LUMO}) = -\Delta E_{M,LUMO} \quad (14b)$$

where $\Delta E_{M,n}$ is given by eq 11a.

The introduction of solvation energies enables the substitution of RP for the ionization potentials and electron affinities[41,42]

$$E^1_{Ox,M} = I_M - 4.44\ \text{eV} + \Delta G_{sol} \quad (15a)$$

$$E^1_{Red,M} = A_M - 4.44\ \text{eV} - \Delta G_{sol} \quad (15b)$$

where 4.44 eV is the absolute potential of a normal hydrogen electrode (NHE) at 298.15 K,[43] $E^1_{Ox,M}$ is the first oxidation potential, $E^1_{Red,M}$ is the first reduction potential (vs NHE), and ΔG_{sol} is the solvation energy for the cation or anion compared to the neutral molecule. Hence,

$$\Delta E^1_{Ox,M} = (E^1_{Ox,M} - E^1_{Ox,Mg}) = \Delta I_M + \Delta\Delta G_{sol} \quad (16a)$$

$$\Delta E^1_{Red,M} = (E^1_{Red,M} - E^1_{Red,Mg}) = \Delta A_M - \Delta\Delta G_{sol} \quad (16b)$$

Solvation energies for large aromatic molecules are generally constant;[41,42,44] therefore it is reasonable to assume $\Delta\Delta G_{sol} \approx 0$. Hence, following eq 11

$$\Delta E^1_{Ox,M} = V^{eff}_{HOMO}\Delta Q_M \approx V^{eff}_{HOMO}(\Gamma\Delta\chi_M + \Lambda\Delta r^c_M) \quad (17a)$$

$$\Delta E^1_{Red,M} = V^{eff}_{LUMO}\Delta Q_M \approx V^{eff}_{LUMO}(\Gamma\Delta\chi_M + \Lambda\Delta r^c_M) \quad (17b)$$

Thus according to eqs 13 and 17 the changes in TE and RP are functions of the change in a central effective charge, which by itself is a function of both the metal electronegativity and covalent radius (mentioned above).

Linear Relationships between Changes in Redox Potentials and Electronic Transition Energies. Koopman theorem states[40,45]

$$E_{M,HOMO\rightarrow LUMO} = I_M - A_M + (J - 2K)_M \quad (18)$$

Using eqs 14−16 and assuming that the exchange (K) and Coulombic (J) integrals as well as solvation energy do not change upon metal variation,[22,28,41,42] we obtain

$$\Delta E_{M,HOMO\rightarrow LUMO} = \Delta E_{M,LUMO} - \Delta E_{M,HOMO} = \Delta E^1_{Ox,M} - \Delta E^1_{Red,M} \quad (19)$$

At the HF level, the left-hand side of eqs 18 and 19 equals the lowest excitation energy. However, this level of theory ignores electron correlation,[40,45,46] which is of prime importance when trying to fit the experimental energies of the electronic transitions in porphyrins with theoretical predictions.

Configuration interactions (CI) partly compensate for the effect of the electron correlation on the energy of the excited states.[39] In particular, the four lowest lying excited states of [M]-BChls are well represented by eqs 12. Here, a correlation effect is introduced, for example, by mixing some $\psi_{M,HOMO-1\rightarrow LUMO+1}$ with $\psi_{M,HOMO\rightarrow LUMO}$. Therefore, E_{M,Q_y} is a linear combination of $E_{M,HOMO\rightarrow LUMO}$ and $E_{M,HOMO-1\rightarrow LUMO+1}$. According to eq 13a

$$\Delta E_{M,Q_y} = C^2_{23}E_{M,HOMO\rightarrow LUMO} + C^2_{14}E_{M,HOMO-1\rightarrow LUMO+1} \quad (20)$$

Substituting eq 19 into eq 20 yields

$$\Delta E_{M,Q_y} = C^2_{23}(\Delta E^1_{Ox,M} - \Delta E^1_{Red,M}) + C^2_{14}E_{M,HOMO-1\rightarrow LUMO+1} \quad (21)$$

$\Delta E_{M,HOMO-1\rightarrow LUMO+1}$ and $\Delta E_{M,HOMO\rightarrow LUMO}$ are proportional to each other since they are determined by the same central potential $V(Q_M, r_a)$. Hence

$$\Delta E_{M,HOMO-1\rightarrow LUMO+1} = \omega\Delta E_{M,HOMO\rightarrow LUMO} = \omega(\Delta E^1_{Ox,M} - \Delta E^1_{Red,M}) \quad (22)$$

Substituting into eq 21 yields

$$\Delta E_{M,Q_y} = (C^2_{23} + \omega C^2_{14})(\Delta E^1_{Ox,M} - \Delta E^1_{Red,M}) = \zeta(\Delta E^1_{Ox,M} - \Delta E^1_{Red,M}) \quad (23)$$

where ω and ζ are proportionality factors. Equation 22, Gouterman's four-orbital model (eq 12) and eq 13a imply that

$$\Delta E_{M,B_y} = C^2_{14}E_{M,HOMO\rightarrow LUMO} + C^2_{23}E_{M,HOMO-1\rightarrow LUMO+1} = (\omega C^2_{23} + C^2_{14})(\Delta E^1_{Ox,M} - \Delta E^1_{Red,M}) \quad (24)$$

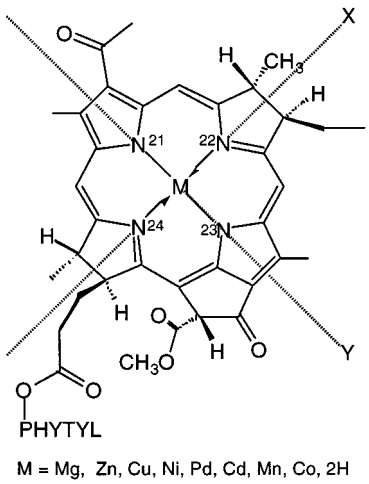

Figure 1. Metal-substituted BChl ([M]-BChl). M = Mg for BChl, 2H for BPhe. The directions of the *X* and *Y* molecular axes are indicated by the dashed lines. Nitrogens are numbered according to IUPAC conventions.[66]

Experimental Section

Syntheses. BChl (Figure 1: M = Mg(II)) and BPhe (Figure 1: M = 2H) were prepared and purified as previously described.[47,48] Synthesis and purification of other [M]-BChls (Figure 1: M = Zn(II), Cu(II), Pd(II), Ni(II), Cd(II)) was according to Hartwich, Fiedor et al.[20−22]

(41) Chen, H. L.; Ellis, P. E. J.; Wijesekera, T.; Hagan, T. E.; Groh, S. E.; Lyons, J. E.; Ridge, D. *J. Am. Chem. Soc.* **1994**, *116*, 1086−1089.
(42) Heinis, T.; Chowdhury, S.; Scott, S. L.; Kebarle, P. *J. Am. Chem. Soc.* **1988**, *110*, 400−407.
(43) Trasatti, S. *Pure Appl. Chem.* **1986**, *58*, 955−966.
(44) Pearson, R. G. *J. Am. Chem. Soc.* **1986**, *108*, 6109−6114.
(45) Michl, J.; Becker, R. *J. Chem. Phys.* **1967**, *46*, 3889−3894.
(46) Salem, L. *The molecular orbital theory of conjugated systems*; W. A. Benjamin Inc.: New York, 1966.
(47) Scherz, A.; Parson, W. W. *Biochim. Biophys. Acta* **1984**, *766*, 666−678.
(48) Struck, A.; Cmiel, E.; Kathender, I.; Schafer, W.; Scheer, H. *Biochim. Biophys. Acta* **1992**, *1101*, 321−328.

Absorption Spectroscopy. A Milton-Roy 1201 spectrophotometer was used for optical absorption spectroscopy. Spectra were recorded in the electrolyte solution prior to electrochemical measurements of the pigments (see below) and in diethyl ether. Standard 10 mm and 0.1 mm quartz cells were used for the measurements in diethyl ether and the electrolyte solution, respectively.

Measurements of Redox Potentials. The [M]-BChls electrochemical oxidation and reduction potentials were measured by linear sweep cyclic voltammetry with a standard three-electrode configuration. A potentiostat (Pine Instruments Co.) and a XY recorder (BBC SE-790) were used for the measurement.

Acetonitrile solution containing 10% dimethylformamide (AN/DMF) and 0.1 M tetrabutylammonium tetrafluoroborate (TBAF) was used as electrolyte solution. The solution was kept over molecular sieves and eluted through an alumina B (ICN) column directly into the electrochemical cell. The dried solution was purged with dry nitrogen for 15 min before a voltammogram was recorded.

A platinum wire cleaned by heating in a flame prior to each measurement was used as a counter electrode. The reference electrode ($Ag|Ag^+$) was a silver wire in a 0.1 M $AgNO_3$ electrolyte solution connected to the main cell compartment by a Luggin capillary sealed with a Vycor frit. The working and counter electrodes were made of platinum. Electrode preparation and sample handling are described elsewhere.[49] The potential was scanned at a rate of 100 mV/s starting in the negative direction. Scan range was set to include both reduction and oxidation potentials in the same sweep. Ferrocene (FeCp) (Aldrich) or bis-biphenyl-chromium (BBCr) (kindly provided by Prof. G. Gritzner, Institute of Inorganic Chemical Technology, University of Linz, Austria) was used as internal reference redox systems.[50,51] The $Ag|Ag^+$ reference electrode potential was measured vs a saturated calomel electrode (SCE) in the electrolyte solution prior to and after each measurement. The potential was found to be 0.37 ± 0.01V vs SCE. Thus, half-wave potentials can be scaled to any aqueous reference system as well as to the absolute potential scale (eq 15). It should be noted, however, that the error because of liquid junction potentials may be as large as 0.2 V.[17,52]

Target Testing Factor Analysis (TTFA). Target testing factor analysis (TTFA) is a multivariate statistical method that helps to determine how many factors describe a set of observables and identifies them in terms of physically significant parameters.[53] Using principal factor analysis (PFA), the experimental data is reproduced by a minimum number of orthogonal eigenvectors of the covariance matrix. These eigenvectors are transformed into physically significant vectors by target transformation using a least-squares method. A detailed description of the mathematical derivation and techniques involved in solving chemical problems with TTFA can be found in ref 53.

Although all of our measurements were carried out in the same solvent, we could not use absolute values for the data analysis. TE values are excited-state energies relative to the ground state of the molecule, whereas RP are measured vs an arbitrary reference system. To overcome this problem, we chose BChl as a reference molecule and analyzed *changes* in TE and RP because of substitution of the central Mg atom by another metal, M ($\Delta E_{M,N} \equiv E_{M,N} - E_{Mg,N}$).

For determining the minimum number of factors, it was assumed that the overall uncertainty in the data matrix due to experimental error is about 0.02 eV. This assumption was based on an error estimate of about 0.01 V in the redox measurements and a spectrophotometer resolution of 1 nm, which corresponds to energy resolution of 0.01 eV in the Soret region and 0.004 and 0.002 eV in the Q_x, Q_y regions, respectively.

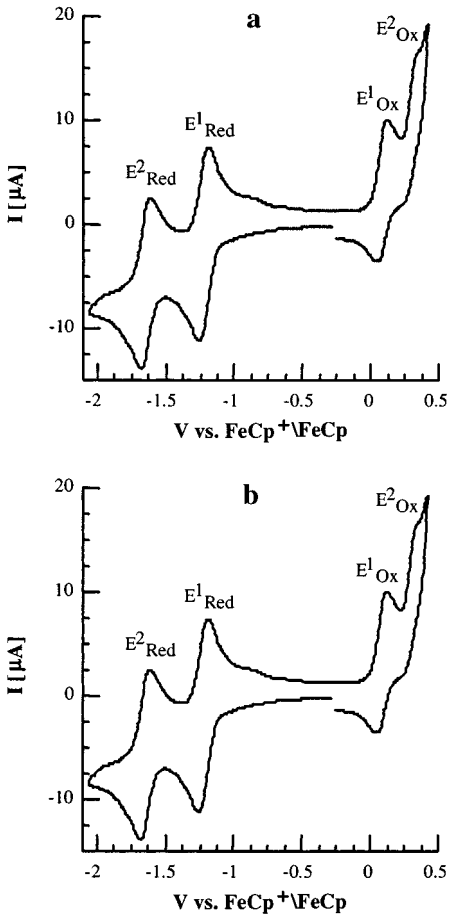

Figure 2. Voltammograms of [Pd]-BChl (a) and [Ni]-BChl (b) in AN/DMF with 0.1 M TBAF. Conditions are described in the Experimental Section.

Target 93M, a program written in Matlab[54] by E. R. Malinowski, was used for the calculations. The program was purchased from E. R. Malinowski at Stevens Institute of technology, Hoboken, NJ.

Results

Redox Potentials. Four-electrode reactions were observed for each [M]-BChl (typical voltammograms are shown in Figure 2). At a scan rate of 100 mV/s, the electrode reactions were reversible, except for the second oxidation of the different [M]-BChls (including BPhe). The RP of BChl and BPhe in AN/DMF (Table 1) are in agreement with respective RP of pentacoordinated BChl and BPhe in other solvents.[17,55]

It is interesting to compare our RP measurement of [M]-BChls in AN/DMF to those measured in THF by Geskes et al.[24] The latter are reported vs Ag|AgCl, an aqueous reference system which is not useful for comparing RP in organic solvents (errors of up to 0.2 V can be expected[17,52]). Hence, the RP values of [M]-BChls in THF were converted to the $FeCp^+$/FeCp internal reference system (Table 2). Apparently, the solvent system strongly affects the reduction potentials and there are notable differences also in the oxidation potentials. A similar trend was observed for other BChl as well as Chl systems.[17,55] The solvent effect on the RP values is not clear at present and is the subject of ongoing study in our laboratory.

Absorption Spectra. The absorption spectra of tetra- and pentacoordinated [M]-BChls in AN/DMF are similar to those

(49) Noy, D. M.Sc. Thesis, Weizmann Institute of Science, 1995.
(50) The difference between the $E_{1/2}$ of $BBCr^+$/BBCr (−1.07 ± 0.01 V vs $Ag|Ag^+$) and $FeCp^+$/FeCp (0.06 ± 0.01 V vs $Ag|Ag^+$) is in agreement with the value of 1.124 ± 0.012 V that was found in 22 other solvents.
(51) Gritzner, G.; Kuta, J. *Pure Appl. Chem.* **1983**, *56*, 461−466.
(52) Diggle, J. W.; Parker, A. J. *Aust. J. Chem.* **1974**, *27*, 1617−1621.
(53) Malinowski, E. R. *Factor Analysis in Chemistry*, 2nd ed.; Wiley: New York, 1991.
(54) Matlab is an interactive matrix computation program by The Mathworks Inc.
(55) Cotton, T. M.; Van Duyne, R. P. *J. Am. Chem. Soc.* **1979**, *101*, 7605−7612.

Table 1. First and Second Half-Wave Oxidation (E^1_{Ox}, E^2_{Ox}) and Reduction (E^1_{Red}, E^2_{Red}) Potentials for [M]-BChls vs $FeCp^+/FeCp$

compd	solvent	E^2_{Ox}	E^1_{Ox}	E^1_{Red}	E^2_{Red}
BChl	AN/DMF	−	−0.11	−1.47	−1.82
	THF[a]	0.32	−0.02	−1.61	−1.95
BPhe	AN/DMF	0.57[b]	0.29	−1.26	−1.66
	THF[a]	0.58	0.29	−1.38	−1.72
Cd-BChl	AN/DMF	0.30[b]	−0.01	−1.39	−1.75
	THF[a]	0.31	0.06	−1.46	−1.83
Cu-BChl	AN/DMF	0.36[b]	0.08	−1.27	−1.65
	THF[a]	0.49	0.05	−1.46	−1.79
Ni-BChl	AN/DMF	0.29[b]	0.08	−1.23	−1.65
	THF[a]	0.39	−0.01	−1.32	−1.68
Pd-BChl	AN/DMF	0.52[b]	0.23	−1.23	−1.66
	THF[a]	0.69	0.29	−1.31	−1.74
Zn-BChl	AN/DMF	0.35[b]	0.00	−1.42	−1.76
	THF[a]	0.40	0.01	−1.52	−1.89

[a] From Geskes et al.[24] Although these authors used Cobaltcenium/Cobaltcene ($CoCp^+/CoCp$) redox couple as an internal reference, redox potentials were reported vs the Ag|AgCl aqueous reference system. We converted these redox potential to the $FeCp^+/FeCp$ reference system using $E_{1/2}(FeCp^+/FeCp) - E_{1/2}(CoCp^+/CoCp) = 1.33$ V[63] and $E_{1/2}(CoCp^+/CoCp)$ vs Ag|AgCl = −0.96 V.[24] [b] Irreversible electrode reaction.

Table 2. Changes in TE and RP of [M]-BChls in AN/DMF Relative to Native (Mg Containing) BChl (3.51, 3.16, 2.16, 1.62 eV for B_y, B_x, Q_x, Q_y, Respectively)

	relative transition energies [eV] and redox potentials [V]					
compd	ΔB_y	ΔB_x	ΔQ_x	ΔQ_y	ΔE^1_{Ox}	ΔE^1_{Red}
BPhe	0.01	0.05	0.21	0.05	0.40	0.21
[Cd]-BChl	−0.06	0.00	−0.03	0.01	0.10	0.08
[Cu]-BChl	0.15	0.01	0.13	0.00	0.19	0.20
[Ni]-BChl	0.22	0.02	0.18	−0.01	0.19	0.24
[Pd]-BChl	0.29	0.08	0.18	0.04	0.34	0.24
[Zn]-BChl	0.00	0.02	0.03	0.02	0.11	0.05

Table 3. Relative Oscillator Strengths of the Major Electronic Transitions of [M]-BChls in DE[64] [a]

compd	$B_{x,y}$ (total), %	Q_x, %	Q_y, %
BChl	70	7 (574)	23 (771)
BPhe	80	7 (524)	14 (750)
[Cd]-BChl	73	6 (575)	21 (761)
[Cu]-BChl	71	7 (535)	22 (767)
[Ni]-BChl	69	6 (531)	25 (780)
[Pd]-BChl	68	7 (527)	26 (754)
[Zn]-BChl	73	7 (556)	20 (759)

[a] Peak positions in nm are given in parentheses.

recorded in THF, pyridine, and DE[22] except for some bandwidth variations. In all four solvents, metal modification had a profound effect on the energies of the Q_x and B_y transitions and a minor effect on their oscillator strengths (Table 3). The only significant exception is BPhe, in which the oscillator strength of the Q_y transition is lower by approximately 10% (~4 Debye^2) relative to BChl. Note that following the previously mentioned coordination criteria[22] the positions of the Q_x band in BChl and [Cd]-BChl (575−580 nm) in AN/DMF and DE reflect pentacoordination of the central metal, whereas the Q_x band of Pd, Cu, and [Ni]-BChl (528−540 nm) indicates tetracoordination. The coordination state of [Zn]-BChl in AN/DMF is somewhat ambiguous since its Q_x transition shifts from 558 nm in DE to 564 nm in AN/DMF. This shift indicates that a mixture of tetra- and penta-coordinated species of [Zn]-BChl exists in AN/DMF.

Correlation between the Electronic Transition Energies, Redox Potentials, and the Electronegativities of the Incorporated Metals. Linear relationships between TE and χ^P_M/r^i_M have been presented in the preceding paper. The corresponding RP values are somewhat better correlated with (χ^P_M) alone (Table 4). However, there is a good linear correlation between the Q_x TE and RP (Table 4). Good linear correlation is also found between the Q_y TE and the difference between the first oxidation and reduction potentials ($E^1_{Ox} - E^1_{Red}$) as predicted by eq 23. This is another experimental support to our assumption that metal substitution does not affect the π-electron distribution; hence, the CI coefficients are unchanged. Nevertheless, the linear correlation between $E^1_{Ox} - E^1_{Red}$ and the B_y TE predicted by eq 24 is not observed. This is probably due to mixing of higher transitions into the B_y excited state, a well-known limit of the four-orbital model.[26]

Preliminary studies have indicated that the linear correlation between the Q_x TE and RP values of [M]-BChls can be applied to other perturbations, even those directed at the molecule periphery.[56] Hence, the position of the Q_x transition can be used as a spectroscopic marker for estimating the RP of in vivo BChls.

Although the simple linear correlations have practical value, more elaborate statistical analysis was needed for testing our theoretical predictions, in particular, the relations between χ_M and χ^P_M and the need to divide χ^P_M by the r^i_M in order to get linear relationships with TE but not with RP.

Target Testing Factor Analysis (TTFA) of Electronic Transition Energies and Redox Potentials. Principal factor analysis determines the minimum number of factors required to describe a database of experimental observations. Target testing examines a proposed correlation between these factors

Table 4. Some Linear Correlations between Redox Potentials and Spectroscopic Transition Energies of [M]-BChls in AN/DMF and Central Metal Electronegativity (Pauling Values)

	linear correlation: $y = a + bx$			
x	y	a	b	R[a]
χ^P_M	E^1_{Ox} [V]	−0.70	0.43	0.97
χ^P_M	E^1_{Red} [V]	−1.85	0.28	0.91
Q_x [eV]	E^1_{Ox} [V]	−2.11	1.26	0.87
Q_x [eV]	E^1_{Red} [V]	−3.45	0.94	0.92
Q_y [eV]	$E^1_{Ox} - E^1_{Red}$ [V]	1.27	0.25	0.97

[a] $R \equiv$ correlation coefficient.

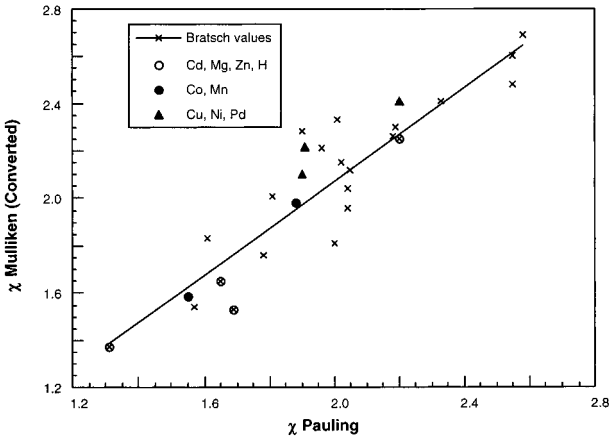

Figure 3. Comparison of published electronegativities with those obtained from target testing factor analysis of M-BChl's redox potentials and transition energies: Mulliken electronegativities for 25 metals converted to Pauling scale according to Bratsch formula[31,57] (×). Predicted values for Cu, Ni, and Pd (▲). Predicted values for Co and Mn (●). The rest of the [M]-BChl central metals are marked with open circles. See text for further explanation.

(56) Noy, D.; Scherz, A. Unpublished data, 1997.

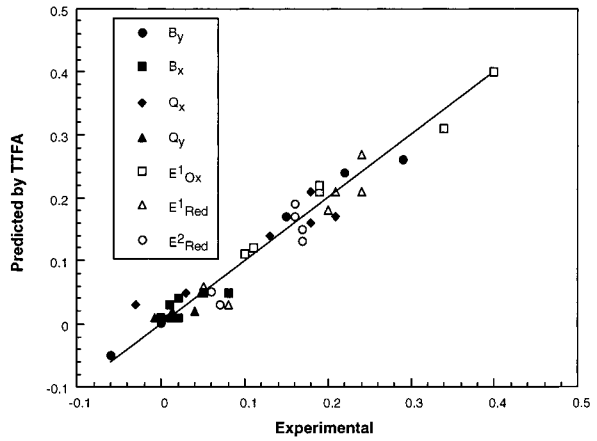

Figure 4. A plot of shifts in electronic transition energies and redox potentials of [M]-BChls relative to BChl, as predicted by TTFA (eq 27), vs experimental data. Straight line represents a 100% match.

Table 5. Central Metal Parameters (Scores) and Their Loading Coefficients Used for the Reproduction of Experimental Electronic Transition Energies and Redox Potentials of [M]-BChls According to eq 26[a]

Scores

M	$\Delta\chi_M$	Δr^c_M
Cd	0.51	0.10
Cu	*2.51*	−0.10
Ni	*2.95*	−0.17
Pd	*3.73*	−0.16
Zn	0.88	0.04
H	3.05	0.15

Loadings

N	$l_{\chi,N}$	$l_{r,N}$
B_y	0.039	−0.72
B_x	0.014	0.03
Q_x	0.056	0.02
Q_y	0.010	0.12
E^1_{Ox}	0.104	0.53
E^1_{Red}	0.071	−0.01
E^2_{Red}	0.054	0.06

[a] Values in italics were predicted by TTFA.

and a set of physical parameters. It does not require a full set of test parameters; it provides predictions for missing ones. The quality of the prediction is an additional criterion for reliable results. This unique feature of TTFA was essential here because of the absence of literature data for Mulliken electronegativities of many transition metals.

Equations 13b and 17 suggest that changes in TE and RP of [M]-BChls reflect modifications of two physical parameters, most probably the metal electronegativity (according to Mulliken) and its covalent radius

$$\Delta E_{M,N} = l_{\chi,N}\Delta\chi_M + l_{r,N}\Delta r^c_M \qquad (26)$$

where $l_{\chi,N}$ and $l_{r,N}$ are the loading coefficients obtained by target transformation[53] and N stands for an observed TE or RP. Indeed, there is a good agreement between the experimental data and those reproduced according to eq 26 using theoretical values and those found in the literature for χ_M and r^c_M (Figure 4 and Table 5). The rms difference between experimental and reproduced data is 0.02 eV, i.e. within the estimated experimental error. Target testing with other parameters such as χ^P_M and r^i_M gave less satisfactory results.

The quality of the predicted Mulliken electronegativities was estimated as follows: Relative electronegativities according to Mulliken were converted to absolute values using eq 6 with $\chi_{Mg} = 4.11$. The resulting values were converted to Pauling electronegativities using the Bratsch formula.[31,57] Although Co and Mn were not included in the database (since they undergo metal centered redox reactions), their electronegativities could be found by extrapolation of the available metal electronegativities (Table 5) and their respective Pauling values.[58] Figure 3 depicts the correlation between the Pauling and Mulliken electronegativities[31] of 25 atoms (after incorporating the predicted values of some atoms that could not be found experimentally). All values fell within the same statistical error, suggesting that the numbers derived here using TTFA faithfully represent the Mulliken electronegativities.

Discussion

Good linear relationships between different properties within a set of molecules indicate structural resemblance.[59] Hence, the correlations found between RP and TE imply that replacement of Mg(II) by Pd(II), Cd(II), Zn(II), Cu(II), and even Ni(II) in BChl does not alter the molecular geometry enough to affect these properties, even though these metals probably have different coordination numbers and there are indications of distortions of the macrocycle in crystallized Ni-porphyrins.[60] Furthermore, our data show that, like unsaturated porphyrins, the free base BPhe fits into the category of metal-substituted BChls (where M = 2 H). If [M]-BChls are structurally similar, the metal effect on the energies of the electronic transitions probably originates in different electrostatic interactions with the π and σ electrons. Many researchers have indicated that for D_{4h} porphyrins such interactions are most likely related to the metal electronegativity.[6,12,13]

Correlation between the Theoretical Predictions and Experimental Results. Figure 4 and Table 5 show that the modifications in RP and TE of metal-substituted BChls can be described as the result of changes in the electronegativity and covalent radius of the central metal. This observed trend agrees with the definition of electronegativity[33−35] within DFT formalism as exemplified by eqs 1−3. However, the coefficients of χ_M and r^c_M in these equations were derived for isolated atoms and recent studies have indicated that they may vary significantly for atoms in a particular molecular environment.[37] Nonetheless, the current application of TTFA requires that the metal electronegativity and covalent radius be kept independent of the particular frontier orbital. Under these conditions, the calculated coefficients for ΔQ_M in eq 7 are given by combining eqs 13b and 17 with eq 26

$$\Gamma_N = \frac{l_{\chi,N}}{V^{eff}_N} \qquad (27a)$$

$$\Lambda_N = \frac{l_{r,N}}{V^{eff}_N} \qquad (27b)$$

It is possible to change V^{eff}_N by varying the CI coefficients for a certain transition or by changing Z_a for a single atom. Thus Γ_N and Λ_N could be optimized to achieve minimum standard deviation between coefficients derived for the different observ-

(57) Bratsch formula for the conversion of Mulliken electronegativities into Pauling scale is $\chi^p = 1.35\sqrt{\chi^m} - 1.37$ where the superscripts m and p refer to Mulliken and Pauling scales, respectively.

(58) Allred, A. L. *J. Inorg. Nucl. Chem.* **1960**, *17*, 215−221.
(59) Sjöström, M.; Wold, S. *Acta Chem. Scand. Ser. B* **1981**, *53*, 537.
(60) Barkigia, K. M.; Thompson, M. A.; Fajer, J. *New. J. Chem.* **1992**, *16*, 599−607.

Table 6. Coefficients of Electronegativity (Γ), the Covalent Radius (Λ), and the Effective Electron Density (V_N^{eff}). See eqs 7, 10, and 13 in Theoretical Considerations for Definition

	B_y	B_x	Q_x	Q_y	E^1_{Ox}	E^1_{Red}	av	%SD[a]	free atom[b]
Γ	0.09	0.14	0.14	0.11	0.15	0.09	0.12	21%	0.49
Λ	−1.72	0.29	0.04	1.32	0.75	−0.02	0.11	938%	0.79
V_N^{eff}[c]	0.42	0.10	0.41	0.09	0.71	0.75			

[a] Relative standard deviation ((SD/av) × 100) in %. [b] Values derived from eq 7 using Alonso's coefficients for free atoms.[35] [c] From eqs 10 and 13. MO coefficients were taken from Scherz et al.[65] $Z_a = 0.8$, $C_{14} = 0.475$, $C_{23} = 0.880$, $C_{13} = 0.810$, $C_{24} = 0.586$. See text for further discussion.

Table 7. Values of ΔQ^o_M and $\Delta q_{M,N}$ Calculated from eq 28

	ΔQ^o_M	$\Delta q_{M,B_y}$	$\Delta q_{M,B_x}$	$\Delta q_{M,Q_x}$	$\Delta q_{M,Q_y}$	$\Delta q_M E^1_{Ox}$	$\Delta q_M E^1_{Red}$
Cd	0.06	−0.17	0.03	0.004	0.13	0.07	−0.002
Cu	0.30	0.17	−0.03	−0.004	−0.13	−0.07	0.002
Ni	0.35	0.30	−0.05	−0.007	−0.23	−0.13	0.003
Pd	0.45	0.27	−0.05	−0.007	−0.21	−0.12	0.003
Zn	0.11	−0.08	0.01	0.002	0.06	0.03	−0.001
H	0.36	−0.26	0.04	0.006	0.20	0.11	−0.002

ables of the same metal. The best result was achieved (Table 6) for $C_{14} = 0.475$, $C_{23} = 0.880$, $C_{13} = 0.810$, $C_{24} = 0.586$, and $Z_a = 0.8$ for all atoms. Under these conditions, $\Gamma_N = \Gamma = 0.12 \pm 0.02$ for all observables, but Λ_N varies significantly. Therefore, ΔQ_M varies slightly for each observable (Table 6) and is given by

$$\Delta Q_{M,N} = \Gamma \Delta \chi_M + \Lambda_N \Delta r^c_M = \Delta Q^o_M + \Delta q_{M,N} \qquad (28)$$

The first term on the right side, ΔQ^o_M, is characteristic of the central metal. It is independent of the molecular environment and proportional to the electronegativity of the metal at a typical valence state. The second term, $\Delta q_{M,N}$, reflects the interaction of the metal atom with the molecular environment. It depends on the overlap between the metal and ligand orbitals and hence changes both with the metal covalent radius (*i.e.*, its typical "size") and the particular orbital environment. Table 7 gives the calculated values of ΔQ^o_M and $\Delta q_{M,N}$. Significant contributions of $\Delta q_{M,N}$ to $\Delta Q_{M,N}$ were observed for B_y, Q_y, and to a lesser extent E^1_{Ox}, whereas $\Delta q_{M,N}$ had minor contributions to the changes of B_x, Q_x, and E^1_{Red}. These observations corresponded with the mode of metal coordination to the central cavity and the π electron density at the ligating nitrogens in [M]-BChl. Two of them, N22 and N24, are of the pyrrolenine type, whereas N21 and N23 are pyrrole-type nitrogens that maintain covalent bonding with the central metal. Stabilization of these bonds brings the metal into a typical divalent state where $\Delta Q_M \approx \Delta Q^o_M$. This is exactly what happens in the *x*-polarized excited states as well as in the LUMO of [M]-BChls, where high electron density is maintained on N22 and N24.[5,7] However, the *y*-polarized transitions as well as the HOMO of the [M]-BChls have low electron density on the pyrrole-type nitrogens, the covalent bond is destabilized, and the metal is not in a typical divalent state. Hence, the metal effective charge at this state should be different from ΔQ^o_M; thus $\Delta q_{M,N}$ becomes more significant.

Although decomposition of ΔQ_M into an inherent property of the central metal and the effect of its molecular environment lacks theoretical support, it agrees well with "chemical intuition". Recent studies have already used the same concept for the electronegativity of atoms in a molecule.[37,61] Still, the full application of this approach is ahead of us, in particular since there is no agreement on the partitioning of molecules.

(61) Komorowski, L.; Lipinski, J. *Chem. Phys.* **1991**, *157*, 45−60.

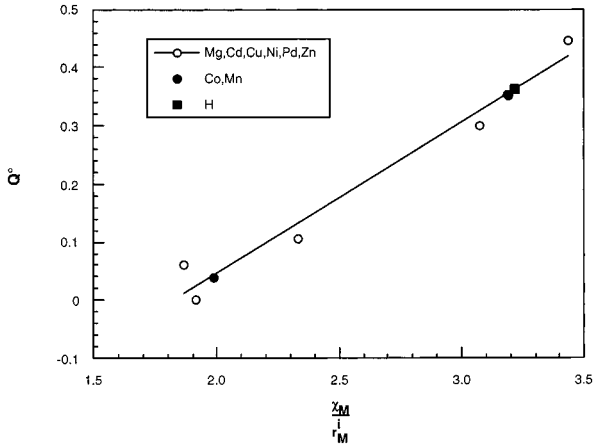

Figure 5. Changes in the typical central metal charge ΔQ^o as a function of M-BChls' χ_M/r^i_M. The correlation coefficient is 0.98 and linear regression (straight line) yielded $\Delta Q^o = 0.26(\chi_M/r^i_M) - 0.48$.

In the previous paper we suggested that scaling χ^P_M by $1/r^i_M$ provides better representation of the metal atom's electronegativity in the rather rigid tetrapyrrole system. The good linear correlation between ΔQ^o_M and χ^P_M/r^i_M (Figure 5) described by

$$\Delta Q^o_M = 0.12\Delta\chi_M = 0.26\frac{\chi^P_M}{r^i_M} - 0.48 \qquad (29)$$

confirms this notion. However, scaling the electronegativity is not enough for a complete description of the interactions between the metal atom and the rest of the molecule. Therefore, using Δq_M as an additional correction factor enables more accurate prediction of experimental data. Note that the present model does not require grouping the metals according to a putative coordination state, since Δq_M accounts for all the environmental effects including the presence of an axial ligand.

The same concepts will probably enable quantifying linear relationships found between RP, TE, and χ^P_M of other porphyrin systems, although the constant parameters may depend on the molecular frame. At the same time, it explains the empirical "stability factor" χ^P_M/r^i_M suggested by Buchler[62] for metal-

(62) Buchler, J. W. In *Porphyrins and Metalloporphyrins*; Smith, K. M., Ed.; Elsevier: Amsterdam, 1975; pp 157−231.

(63) Shalev, H.; Evans, D. H. *J. Am. Chem. Soc.* **1989**, *111*, 2667−2674.

substituted porphyrins: the binding energy to the porphyrin macrocycle (the ligand) increases with the effective charge of the central metal. In light of this argumentation, the metal size alone may become a minor factor in determining the complex stability.

It is tempting to generalize the relationships between ΔQ_M^o and χ_M^p/r_M^i to other metals and ligand systems. However, the validity of such a generalization requires further support.

Conclusions and Perspectives

(1) The presented data and accompanying theoretical considerations support the approach to electronegativity using DFT.

(2) Incorporation of metals into porphyrins and, in particular, BChls enables straightforward calculation of their electronegativity and its scaling into positive charge units.

(3) The experimental variations in RP and TE of [M]-BChls are determined by electrostatic interactions between the effective charge in the center of the molecule and the electron densities in the frontier molecular orbitals. Hence, it is subjected to both ligand effect (via axial coordination) and ring substitution effects (via the M-N σ bonding). Therefore, the electrostatic model may account for the effect of ligation and site-directed mutagenesis on the BChl's TE and RP modifications. A similar model is expected to explain previously reported data in other metal-substituted porphyrin systems. The successful simulation suggests that the orbitals can be considered "stiff": there was no significant change in the electron densities of the frontier molecular orbitals after metal substitution, but only in their HF energies. The suggested methodology should be applicable to analyze the TE and RP of in vivo BChls and Chls in their native environment and their changes upon site-directed mutagenesis and replacement with modified pigments. It is also expected to help in understanding the properties of complexes of unknown structure. Conversely, by systematic modification of a particular site and analysis of the results as described here, it should be possible to estimate effective charges and electronegativities of amino acid residues in the protein domain.

Acknowledgment. We are grateful to Prof. I. Rubinstein and Dr. Y. Golan from the Department of Materials and Interfaces at the Weizmann Institute of Science for their guidance in performing the electrochemical measurements. We are indebted to Prof. J. R. Norris from the Department of Chemistry at the University of Chicago for critical reading and helpful discussions. This research was supported by the DFG grant Sche 140/9-3 and the Willstätter-Avron-Minerva Foundation for Photosynthesis.

JA970875M

(64) Relative oscillator strengths are estimated by integrating each transition band and dividing the result by the sum of integrated bands of the major transitions, namely, Q_y, Q_x, and Soret bands. Since the B_y and B_x transition bands are not well resolved, the Soret band is integrated as a whole. Transition bands at higher energy than the Soret are not considered. The accuracy of integration is subjective to (a) overlap of higher energy transitions with the Soret band; (b) baseline deviation. The error of the oscillator strength is ±5%.

(65) Scherz, A.; Fisher, J. R. E.; Braun, P. In *Reaction Center of Photosynthetic Bacteria*; Michel-Beyerle, M. E., Ed.; Springer-Verlag: Berlin, 1990; pp 377−388.

(66) Hynninen, P. H. In *Chlorophylls*; Scheer, H., Ed.; CRC Press: Boca Raton, FL, 1991; pp 145−209.